

# Symmetry-Protected $\alpha$ -Attractor Hybrid Inflation in Supergravity and Constraints from ACT DR6 and DESI DR2

Swapnil Kumar Singh  <sup>1\*</sup>

<sup>1</sup>*B.M.S. College of Engineering, Bangalore, Karnataka, 560019, India.*

We present a symmetry-protected supergravity realization of hybrid  $\alpha$ -attractor inflation with a constant sequestered uplift. The model achieves an exact analytic embedding of the attractor geometry while maintaining vacuum stability and radiative control. The uplift, generated by a hidden Stückelberg  $U(1)_D$  sector, preserves the inflaton dynamics and provides an independent handle on the post-inflationary vacuum energy. The framework yields precise next-to-leading-order predictions for the scalar spectral tilt and tensor amplitude, fully consistent with current ACT DR6, DESI DR2, and Planck data. Radiative and geometric corrections remain exponentially suppressed, ensuring the robustness of the inflationary trajectory. This construction offers a minimal, UV-complete, and testable benchmark for embedding  $\alpha$ -attractor inflation in supergravity, with tensor modes potentially observable by LiteBIRD and CMB-S4.

**Keywords:** Supergravity,  $\alpha$ -Attractors, Hybrid Inflation, CMB constraints

## Contents

I. Introduction	1
II. Supergravity construction	2
III. Background dynamics and the exact $N$ -mapping	7
IV. Perturbations and quantum consistency	9
V. Post-inflationary dynamics and vacuum structure	10
VI. Comparison with observations and parameter dependence	11
VII. Conclusion	12
References	17

## I. Introduction

The inflationary paradigm provides a compelling description of the early Universe, offering a minimal and empirically successful mechanism for generating a spatially flat, homogeneous cosmos with a nearly Gaussian, adiabatic spectrum of scalar perturbations whose tilt is close to scale invariance [1–3]. Precision measurements of the cosmic microwave background (CMB), especially by the *Planck* satellite, have confirmed these predictions by tightly constraining the amplitude, spectral tilt, and tensor-to-scalar ratio of primordial perturbations [4, 5].

Forthcoming observations will further sharpen these tests. The Simons Observatory [6] and the LiteBIRD satellite [7] aim to probe CMB  $B$ -modes with unprecedented sensitivity, while space-based gravitational-wave missions such as LISA, DECIGO, and BBO [8–16] target the stochastic background of inflationary gravitational waves. The recent confirmation of a stochastic signal by Pulsar Timing Array collaborations [17–20] has intensified interest in models that could yield such backgrounds, though canonical single-field slow-roll scenarios alone are unlikely to explain them [21, 22]. Meanwhile, the latest Atacama Cosmology Telescope results [23, 24], combined with DESI data [25], favor a slightly higher scalar spectral index,  $n_S = 0.9743 \pm 0.0034$ , in mild ( $\sim 2\sigma$ ) tension with *Planck*, prompting renewed interest in inflationary models that can accommodate such shifts [26–60].

Hybrid inflation [61] occupies a special place in this landscape. Its dynamics proceed along a quasi-flat valley in a multi-field potential and terminate when an orthogonal “waterfall” field becomes tachyonic, ending inflation abruptly.

This built-in exit mechanism avoids ambiguities in slow-roll termination and enables controlled symmetry breaking in the post-inflationary phase. Embedding hybrid inflation in supergravity (SUGRA) introduces the familiar  $\eta$ -problem: order-one corrections from the Kähler curvature can spoil flatness [62–65]. The framework of  $\alpha$ -attractors provides a geometric solution [66–70]. Here the inflaton spans a hyperbolic manifold (Poincaré disk or half-plane), whose negative curvature stretches field space near the boundary, flattening a wide class of potentials after canonical normalization. The resulting E- and T-models predict  $n_s \simeq 1 - 2/N$  and  $r \simeq \mathcal{O}(\alpha)/N^2$ , exhibiting remarkable universality and UV insensitivity.

Recent works [71] have analyzed the interplay between geometric stabilization, attractor dynamics, and F- and D-term contributions in such settings. These developments highlight the importance of models in which uplift sectors and waterfall dynamics are sequestered, maintaining analytic control while preserving attractor predictions.

In this work we construct a SUGRA realization that merges hybrid inflation with  $\alpha$ -attractor geometry, yielding an exact E-model plateau potential and a controlled hybrid exit. The model contains three chiral multiplets  $(T, S, \Psi, \bar{\Psi})$ —the inflaton modulus  $T$ , a stabilizer  $S$ , and a pair of oppositely charged waterfall fields  $(\Psi, \bar{\Psi})$  under a gauged  $U(1)_X$ —together with a sequestered Stückelberg  $U(1)_D$  sector that generates a constant uplift along the inflationary valley. The inflaton corresponds to the canonically normalized real part of  $T$  on the half-plane, while the  $T$ -dependent supersymmetric mass of the waterfall pair triggers the exit when one scalar becomes tachyonic. We derive the exact background dynamics, the  $N-\phi$  relation in the presence of uplift, and the full mass spectrum and stability conditions. Next-to-leading-order predictions for  $(n_s, r)$  are computed within the Hubble-flow hierarchy [72–75], and quantum stability is examined through Coleman–Weinberg corrections [76–78]. Our analysis shows that the model preserves the universal  $\alpha$ -attractor predictions for  $n_s$ , naturally suppresses the tensor amplitude through a sequestered de-Sitter uplift, and remains consistent with the latest CMB data. We adopt reduced Planck units  $M_{\text{Pl}}=1$  unless otherwise stated.<sup>1</sup>

The remainder of this paper is organized as follows. In Section II, we present the full supergravity construction, including the Kähler and superpotential structure, the gauge sectors, and the sequestered Stückelberg uplift mechanism. Section III derives the exact background dynamics and the analytical  $N-\phi$  mapping in the presence of a constant uplift. In Section IV, we compute the inflationary perturbations using the Hubble-flow hierarchy, obtaining next-to-leading-order predictions for the spectral index and tensor amplitude. Section V discusses the post-inflationary dynamics, including reheating, stabilization, and vacuum structure. In Section VI, we compare the theoretical predictions with current CMB observations and analyze the dependence on model parameters. Finally, Section VII summarizes our results and outlines potential extensions of the framework.

## II. Supergravity construction

### Field content, Kähler geometry, and superpotential

We begin by specifying the chiral field content of the inflationary sector. The model contains four chiral multiplets: the inflaton modulus  $T$ , a stabilizer field  $S$ , and a pair of waterfall multiplets  $\Psi$  and  $\bar{\Psi}$  with opposite charges  $\pm 1$  under an Abelian gauge group  $U(1)_X$ . The inflaton modulus  $T$  parametrizes a hyperbolic Kähler manifold corresponding to the Poincaré half-plane, whose curvature is controlled by the parameter  $\alpha$  [66, 79, 80]. The hyperbolic geometry provides the essential flattening of the potential characteristic of  $\alpha$ -attractors and ensures the robustness of slow-roll inflation against higher-order corrections.

We choose a factorized but nontrivial frame function that places all fields within the same conformal prefactor:

$$K = -3\alpha \ln(T + \bar{T}) + (T + \bar{T})^{-3\alpha} (|S|^2 + |\Psi|^2 + |\bar{\Psi}|^2). \quad (1)$$

Here  $(T + \bar{T})^{-3\alpha}$  acts as a universal conformal prefactor, ensuring that the kinetic metrics of all matter fields scale uniformly with the inflaton modulus. This choice keeps Kähler invariance manifest and mixes the inflaton and matter geometries only through the overall frame factor.

This form maintains manifest Kähler invariance and induces a nontrivial mixing between the inflaton geometry and the matter fields through the  $(T + \bar{T})^{-3\alpha}$  factor. Along the inflationary valley  $S = \Psi = \bar{\Psi} = 0$  with  $T = \bar{T} > 0$ , the

---

<sup>1</sup> Canonical scalar fields have mass dimension 1; the holomorphic superpotential  $W$  has dimension 3; parameters such as  $V_0 = \mu^2$  carry dimension 4; and the Yukawa-like parameter  $g$  in  $W$  has dimension 1, while gauge couplings  $g_X$  and quartic  $\lambda$  are dimensionless.

nonvanishing components of the Kähler metric and its inverse are

$$K_{T\bar{T}} = \frac{3\alpha}{(T + \bar{T})^2}, \quad K_{S\bar{S}} = K_{\Psi\bar{\Psi}} = K_{\bar{\Psi}\bar{\Psi}} = (T + \bar{T})^{-3\alpha}, \quad K^{S\bar{S}} = K^{\Psi\bar{\Psi}} = K^{\bar{\Psi}\bar{\Psi}} = (T + \bar{T})^{3\alpha}, \quad (2)$$

and hence  $e^K = (T + \bar{T})^{-3\alpha}$ . The structure of (2) leads to the remarkable cancellations

$$e^K K^{S\bar{S}} = 1, \quad e^K K^{\Psi\bar{\Psi}} = e^K K^{\bar{\Psi}\bar{\Psi}} = 1, \quad (3)$$

which eliminate any residual  $T$ -dependence from the stabilizer F-term energy density and from the supersymmetric masses of the waterfall multiplets along the inflationary trajectory. This property guarantees that the potential energy is purely determined by the holomorphic structure of the superpotential and not by the varying inflaton frame factor. On the real slice  $T = \bar{T} > 0$ , we have  $T + \bar{T} = 2 \operatorname{Re} T$ , which we use implicitly in what follows.

The holomorphic superpotential is chosen as

$$W = S \mu (1 - T^{-1}) + g (1 - T^{-1}) \Psi \bar{\Psi}, \quad (4)$$

which is manifestly gauge invariant under  $U(1)_X$ . The first term provides an  $\alpha$ -attractor-type E-model potential for the inflaton when  $S$  acts as a stabilizer, while the second term assigns a  $T$ -dependent supersymmetric mass to the waterfall fields. The coupling  $g$  controls the critical field value at which the hybrid transition occurs. The combination  $(1 - T^{-1})$  ensures that the supersymmetric vacuum lies at  $T = 1$  where both F- and D-terms vanish.

### F-term and the inflationary valley

In  $\mathcal{N} = 1$  supergravity, the F-term scalar potential is given by [81, 82]

$$V_F = e^K \left( K^{I\bar{J}} D_I W D_{\bar{J}} \bar{W} - 3|W|^2 \right), \quad D_I W \equiv \partial_I W + (\partial_I K) W, \quad (5)$$

where the indices  $I, \bar{J}$  run over all chiral multiplets. Evaluating (5) along the real inflationary valley  $S = \Psi = \bar{\Psi} = 0$ , one finds

$$W|_{\text{val}} = 0, \quad D_T W|_{\text{val}} = 0, \quad D_S W|_{\text{val}} = \mu(1 - T^{-1}). \quad (6)$$

Therefore, the F-term energy density simplifies to

$$V_F|_{\text{val}} = e^K K^{S\bar{S}} |D_S W|^2 = \mu^2 |1 - T^{-1}|^2, \quad (7)$$

which is independent of  $T$  through the cancellation (3). This exact form realizes the characteristic  $\alpha$ -attractor plateau once the field is canonically normalized.

### Sequestered constant uplift from a Stueckelberg sector

To generate a positive cosmological constant during inflation without altering the inflaton geometry, we introduce a sequestered  $U(1)_D$  gauge sector coupled to a Stueckelberg chiral multiplet  $\Sigma$ . This sector gauges an axionic shift symmetry of  $\Sigma$ :

$$\delta\Sigma = iq\Lambda, \quad K_{\text{Stk}} = k(\Sigma + \bar{\Sigma} + qV_D), \quad f_D = \text{constant}. \quad (8)$$

The corresponding Killing potential is

$$\mathcal{P}_D = -q \partial_{\Sigma + \bar{\Sigma}} k|_{\langle\Sigma\rangle} \equiv \xi_{\text{eff}} = \text{constant}, \quad (9)$$

producing a constant D-term contribution

$$V_D = \frac{g_D^2}{2} \xi_{\text{eff}}^2 \equiv V_{\text{up}}. \quad (10)$$

The total Kähler potential and gauge kinetic functions are assumed to factorize as

$$K = K_{\text{infl}}(T, S, \Psi, \bar{\Psi}) + K_{\text{Stk}}(\Sigma + \bar{\Sigma}), \quad f = \text{diag}(f_{\text{infl}}(T), f_D), \quad (11)$$

ensuring that the Stueckelberg sector is fully sequestered from the inflaton dynamics. Consequently, integrating out  $\Sigma$  and the  $U(1)_D$  vector simply adds a constant positive uplift  $V_{\text{up}}$  to the inflationary potential without introducing backreaction [83, 84]. The full valley potential becomes

$$V(\phi, 0) = U(\phi) + V_{\text{up}}, \quad (12)$$

where  $U(\phi)$  is the E-model potential derived below. This uplift mechanism is minimal, stable, and fully consistent with the  $\alpha$ -attractor geometry.

### Canonical normalization and the E-model plateau

Along the inflationary trajectory, the kinetic term for the modulus  $T$  is

$$\mathcal{L}_{\text{kin}} = K_{T\bar{T}} \partial T \partial \bar{T} = \frac{3\alpha}{(T + \bar{T})^2} \partial T \partial \bar{T}. \quad (13)$$

For  $T = \bar{T} > 0$ , we define the canonically normalized inflaton  $\phi$  through the exponential map

$$T = e^{\beta\phi}, \quad \beta = \sqrt{\frac{2}{3\alpha}}, \quad (14)$$

which yields a canonical kinetic term  $\mathcal{L}_{\text{kin}} = \frac{1}{2}(\partial\phi)^2$ . Substituting (14) into (7), one obtains the exact E-model plateau potential

$$U(\phi) = V_0 (1 - e^{-\beta\phi})^2, \quad V_0 = \mu^2, \quad (15)$$

which asymptotes to  $U \rightarrow V_0$  for  $\phi \rightarrow +\infty$ . The resulting potential combines the universal predictions of  $\alpha$ -attractors with the microphysical control provided by a supergravity embedding.

### Hybrid sector, mass spectrum, and the critical point

The inflationary phase ends through a tachyonic instability of the waterfall fields  $\Psi$  and  $\bar{\Psi}$ , which are charged under  $U(1)_X$  with gauge coupling  $g_X$ . The D-term potential is

$$V_X = \frac{g_X^2}{2} (|\Psi|^2 - |\bar{\Psi}|^2 - v_D^2)^2, \quad (16)$$

where  $v_D$  parameterizes the Fayet–Iliopoulos contribution or spontaneous breaking scale. The supersymmetric mass of the waterfall pair arises from the  $T$ -dependent term in (4),

$$m_F^2(\phi) = g^2 |1 - e^{-\beta\phi}|^2. \quad (17)$$

The scalar components split due to the D-term and SUGRA curvature, giving

$$m_{\pm}^2(\phi) = g^2 |1 - e^{-\beta\phi}|^2 \pm g_X^2 v_D^2 + \Delta m^2(\phi), \quad (18)$$

where  $\Delta m^2(\phi)$  encodes Hubble-induced curvature corrections,

$$\Delta m^2(\phi) = -R_{\Phi\bar{\Phi}S\bar{S}} F^S \bar{F}^{\bar{S}}, \quad F^S = e^{K/2} K^{S\bar{S}} D_S W. \quad (19)$$

For the Kähler potential (1), the relevant Riemann tensor component is

$$R_{\Phi\bar{\Phi}S\bar{S}} = 3\alpha (T + \bar{T})^{-6\alpha}. \quad (20)$$

Using  $e^K K^{S\bar{S}} = 1$  and  $U = e^K K^{S\bar{S}} |D_S W|^2$ , we obtain

$$\boxed{\Delta m^2(\phi) = -3\alpha (T + \bar{T})^{-6\alpha} U(\phi) = -\tilde{c} U(\phi) e^{-\sqrt{24\alpha}\phi}, \quad \tilde{c} = 3\alpha 2^{-6\alpha}.} \quad (21)$$

Stability of the inflationary valley requires  $m_{\pm}^2(\phi) > 0$ . The critical field value  $\phi_c$  is defined by  $m_-^2(\phi_c) = 0$ , which yields

$$g |1 - e^{-\beta\phi_c}| = g_X v_D \implies \phi_c = \frac{1}{\beta} \ln \left( \frac{1}{1 - \frac{g_X v_D}{g}} \right), \quad 0 < \frac{g_X v_D}{g} < 1. \quad (22)$$

For  $\phi > \phi_c$ , both scalars are stabilized, while at  $\phi = \phi_c$  the lighter mode becomes tachyonic, triggering the waterfall transition and ending inflation.

### Promptness of the waterfall and the inflaton phase

Close to the critical point, the lightest scalar mass behaves as  $m_-^2(\phi) \simeq A(\phi - \phi_c)$  with  $A > 0$ . Using  $d\phi/dN = -U'/V$  and  $V = U + V_{\text{up}}$ , the exit is prompt if

$$\boxed{\left| \frac{m_-}{H} \right| \Big|_{\phi_c} \gtrsim \mathcal{O}(1), \quad \text{or equivalently} \quad g |1 - e^{-\beta\phi_c}| \gtrsim \mathcal{O}(1) \times H(\phi_c).} \quad (23)$$

This condition ensures a fast tachyonic instability and avoids prolonged multi-field evolution after the critical point.

The imaginary part of the modulus  $T$  is generally light during inflation. Writing  $T = u e^{i\vartheta}$  with  $u = e^{\beta\phi}$ , the potential becomes

$$U(\phi, \vartheta) = \mu^2 \left( 1 - \frac{2 \cos \vartheta}{u} + \frac{1}{u^2} \right) = U(\phi, 0) + \mu^2 \frac{\vartheta^2}{u} + \mathcal{O}(\vartheta^4), \quad (24)$$

leading to a canonically normalized mass

$$m_{\text{Im } T}^2 \simeq \frac{4}{3\alpha} \frac{\mu^2}{u}, \quad \frac{m_{\text{Im } T}^2}{H^2} \simeq \frac{4}{\alpha u} \frac{V_0}{V_0 + V_{\text{up}}} \ll 1 \quad (u \gg 1). \quad (25)$$

Thus the imaginary component of  $T$  remains light on the plateau, and the system is mildly two-field unless additional stabilization terms are included (for instance, a small  $T$ -dependent correction in  $K$  or  $W$ ). The predictions derived in later sections correspond to the single-field, adiabatic trajectory.

The full scalar potential of the theory consists of both F-term and D-term contributions arising from the combined inflaton–stabilizer–waterfall sector and the sequestered Stueckelberg uplift,

$$V_{\text{tot}} = V_F + V_X + V_D, \quad (26)$$

where  $V_F$  is given by (5),  $V_X$  by the  $U(1)_X$  gauge interaction, and  $V_D$  by the constant Stueckelberg uplift (10). The respective roles of these terms are distinct:

- ×  $V_F$  drives inflation through the  $\alpha$ -attractor plateau potential.
- ×  $V_X$  controls the hybrid transition and stabilizes the charged fields during inflation.
- ×  $V_D$  provides a constant positive offset, lifting the potential energy density without altering its slope or curvature along the inflaton direction.

Hence the energy hierarchy during inflation satisfies

$$V_F \simeq U(\phi) \gg V_X|_{\text{val}} = 0, \quad V_D = V_{\text{up}} = \text{constant}, \quad (27)$$

and the inflationary energy scale is  $V_{\text{inf}} \simeq V_0 + V_{\text{up}}$ .

Substituting (15) and (10) into (26) along the valley ( $S = \Psi = \bar{\Psi} = 0$ ), we obtain

$$V_{\text{tot}}(\phi) = V_0 (1 - e^{-\beta\phi})^2 + V_{\text{up}}, \quad (28)$$

where  $V_0 = \mu^2$  and  $\beta = \sqrt{2/(3\alpha)}$ . This form is exact to all orders in supergravity and provides an analytical benchmark for studying hybrid  $\alpha$ -attractor dynamics. The constant  $V_{\text{up}}$  controls the overall height of the potential and modifies the relative scale between the inflationary plateau and the post-inflationary vacuum.

In the limit  $V_{\text{up}} \rightarrow 0$ , one recovers the standard E-model potential with a supersymmetric Minkowski vacuum at  $T = 1$ . For  $V_{\text{up}} > 0$ , the minimum remains at  $T = 1$  but with residual positive energy  $V_{\text{up}}$ , which can be canceled by an additional small negative contribution from a hidden sector if one wishes to achieve a zero cosmological constant after reheating.

The slow-roll dynamics are governed by the first and second Hubble-flow parameters,

$$\epsilon = \frac{1}{2} \left( \frac{V'(\phi)}{V(\phi)} \right)^2, \quad \eta = \frac{V''(\phi)}{V(\phi)}, \quad (29)$$

where primes denote derivatives with respect to  $\phi$ . Using (28), we obtain

$$V'(\phi) = 2\beta V_0 e^{-\beta\phi} (1 - e^{-\beta\phi}), \quad (30)$$

$$V''(\phi) = 2\beta^2 V_0 e^{-\beta\phi} (2e^{-\beta\phi} - 1). \quad (31)$$

The resulting slow-roll parameters are

$$\epsilon(\phi) = 2\beta^2 \left( \frac{V_0}{V_0(1 - e^{-\beta\phi})^2 + V_{\text{up}}} \right)^2 e^{-2\beta\phi} (1 - e^{-\beta\phi})^2, \quad (32)$$

$$\eta(\phi) = 2\beta^2 \frac{V_0 e^{-\beta\phi} (2e^{-\beta\phi} - 1)}{V_0(1 - e^{-\beta\phi})^2 + V_{\text{up}}}. \quad (33)$$

In the asymptotic regime  $\phi \gg 1/\beta$ , one finds

$$\epsilon \simeq \frac{3\alpha}{4N^2} \left( \frac{V_0}{V_0 + V_{\text{up}}} \right)^2, \quad \eta \simeq -\frac{1}{N}, \quad (34)$$

leading to the attractor predictions

$$n_s \simeq 1 - \frac{2}{N_*}, \quad r \simeq \frac{12\alpha}{N_*^2} \left( \frac{V_0}{V_0 + V_{\text{up}}} \right)^2. \quad (35)$$

The uplift therefore suppresses  $r$  by a factor  $(V_0/(V_0 + V_{\text{up}}))^2$  without affecting the spectral tilt, offering a controlled mechanism to reduce tensor modes while preserving the universal  $\alpha$ -attractor prediction for  $n_s$ .

The model is characterized by five essential parameters:

$$\{\alpha, \mu, g, g_X, V_{\text{up}}\}. \quad (36)$$

Among these,  $\alpha$  determines the curvature of the inflaton manifold and the leading-order scaling of  $(n_s, r)$ ,  $\mu$  sets the inflationary energy scale, and  $V_{\text{up}}$  modulates the tensor amplitude. The couplings  $g$  and  $g_X$  govern the hybrid transition, controlling the critical field value  $\phi_c$  and the speed of the waterfall. For phenomenologically viable scenarios consistent with *Planck*, ACT, and DESI data, one typically finds

$$\alpha \lesssim 1, \quad g, g_X \sim 10^{-3} - 10^{-2}, \quad V_{\text{up}} \lesssim (0.1 - 0.3)V_0, \quad (37)$$

yielding  $n_s \simeq 0.965 - 0.975$  and  $r \simeq 10^{-4} - 10^{-3}$ . The model thus naturally accommodates the observed CMB spectral tilt and lies within the sensitivity range of future B-mode experiments.

Finally, radiative corrections from the Coleman–Weinberg potential,

$$V_{\text{CW}} = \frac{1}{64\pi^2} \sum_i (-1)^{F_i} m_i^4(\phi) \ln \frac{m_i^2(\phi)}{\Lambda^2}, \quad (38)$$

remain exponentially suppressed on the plateau due to  $m_i^2(\phi) \sim e^{-2\beta\phi}$ , ensuring radiative stability for all perturbative couplings  $g \lesssim 10^{-2}$ . The inflaton potential (28) thus retains its exact analytical form even after including loop corrections, establishing a fully consistent and predictive framework for supergravity hybrid  $\alpha$ -attractor inflation.

### III. Background dynamics and the exact $N$ -mapping

#### Field evolution with constant uplift

To describe the inflaton dynamics, we work in terms of the number of e-folds  $N \equiv \ln a$  as the time variable. The background field equation in the slow-roll approximation reads

$$\frac{d\phi}{dN} = -\frac{V_{,\phi}}{V} = -\frac{U'(\phi)}{U(\phi) + V_{\text{up}}}, \quad (39)$$

where  $U(\phi)$  is the  $\alpha$ -attractor E-model potential given in Eq. (15), and  $V_{\text{up}}$  is the constant sequestered uplift introduced in Sec. II. This form remains exact in the slow-roll regime and correctly captures the field evolution on the plateau.

It is convenient to trade the canonical field  $\phi$  for the variable

$$u \equiv e^{\beta\phi}, \quad \beta \equiv \sqrt{\frac{2}{3\alpha}}, \quad (40)$$

in terms of which the potential and its derivative take the form

$$U(u) = V_0 \left(1 - \frac{2}{u} + \frac{1}{u^2}\right), \quad U'(\phi) = 2\beta V_0 \frac{u-1}{u^2}. \quad (41)$$

The differential relation between  $u$  and  $N$  then becomes

$$\frac{du}{dN} = \beta u \frac{d\phi}{dN} = -\frac{2\beta^2 V_0 (u-1)}{u [U(u) + V_{\text{up}}]}. \quad (42)$$

This exact first-order equation governs the evolution of the field on the plateau in the presence of a constant uplift. It generalizes the standard  $\alpha$ -attractor flow by introducing an effective suppression factor  $\sim (U + V_{\text{up}})^{-1}$  that reduces the velocity of the inflaton for fixed  $V_0$ .

#### Exact analytic $N$ - $\phi$ mapping

The number of e-folds accumulated as the field evolves from a given value  $\phi$  to the end of inflation (at  $\phi_c$ ) is

$$N(\phi; \phi_c) = \int_{\phi_c}^{\phi} \frac{V}{V_{,\phi}} d\phi = \int_{u_c}^u \frac{V(u)}{V'(u)} \frac{du}{\beta u}. \quad (43)$$

Substituting Eqs. (42) and (15) and performing the integration yields the exact closed-form expression

$$N(\phi; \phi_c) = \frac{1}{2\beta^2 V_0} \left[ (V_0 + V_{\text{up}})(u_c - u) + V_{\text{up}} \ln \frac{u_c - 1}{u - 1} - V_0 \ln \frac{u_c}{u} \right], \quad (44)$$

where  $u = e^{\beta\phi}$  and  $u_c = e^{\beta\phi_c}$  denote the field values at the time of evaluation and at the critical point, respectively.

Equation (44) provides an exact analytic  $N$ -mapping for the hybrid  $\alpha$ -attractor with constant uplift. The first term represents the dominant linear scaling of  $N$  with  $u$  (and hence with  $\phi$ ), while the logarithmic terms encode subleading geometric corrections due to the hyperbolic field-space curvature and the uplift contribution.

**Plateau limit and approximate mapping.** In the asymptotic regime  $u \gg 1$  (corresponding to the flat portion of the potential) and  $u \gtrsim u_c$ , the logarithmic corrections in (44) are small compared to the leading term. Expanding to first order in  $1/u$  yields

$$e^{\beta\phi_N} \simeq e^{\beta\phi_c} + \frac{2\beta^2 V_0}{V_0 + V_{\text{up}}} N = e^{\beta\phi_c} + \frac{4}{3\alpha} \frac{V_0}{V_0 + V_{\text{up}}} N. \quad (45)$$

For a strongly plateau-like potential with  $V_{\text{up}} \ll V_0$  and  $e^{\beta\phi_c} \ll e^{\beta\phi_N}$ , the mapping simplifies to the familiar attractor relation

$$e^{\beta\phi_N} \simeq \frac{4N}{3\alpha}. \quad (46)$$

This expression is accurate to better than 1% for  $N \gtrsim 40$  and provides an excellent approximation for all phenomenologically relevant regimes. The uplift term thus rescales the effective slope of  $\phi(N)$  without altering the logarithmic shape of the potential.

The effect of a positive uplift  $V_{\text{up}} > 0$  is twofold:

- (a) It **slows down** the evolution of  $\phi$  for fixed  $N$ , since the denominator in Eq. (39) increases, effectively flattening the potential further.
- (b) It **extends the inflationary phase** by increasing the number of e-folds generated for a given field excursion, thereby suppressing the tensor amplitude  $r$ .

This modification preserves the universal attractor scaling for  $n_s$ , while reducing  $r$  by the factor  $(V_0/(V_0 + V_{\text{up}}))^2$ , as derived below.

### Slow-roll parameters and leading predictions

The potential slow-roll parameters are defined in terms of  $V = U + V_{\text{up}}$  as

$$\epsilon_V = \frac{1}{2} \left( \frac{V_{,\phi}}{V} \right)^2, \quad \eta_V = \frac{V_{,\phi\phi}}{V}. \quad (47)$$

Using the explicit expressions for  $U(u)$  and its derivatives,

$$U'(\phi) = 2\beta V_0 \frac{u-1}{u^2}, \quad U''(\phi) = 2\beta^2 V_0 \frac{2-u}{u^2}, \quad (48)$$

one obtains

$$\epsilon_V = \frac{2\beta^2 V_0^2}{(U + V_{\text{up}})^2} \frac{(u-1)^2}{u^4}, \quad \eta_V = \frac{2\beta^2 V_0}{U + V_{\text{up}}} \left( \frac{2}{u^2} - \frac{1}{u} \right). \quad (49)$$

In the large- $u$  regime, these reduce to

$$\epsilon_V \simeq 2\beta^2 \left( \frac{V_0}{V_0 + V_{\text{up}}} \right)^2 e^{-2\beta\phi}, \quad \eta_V \simeq -2\beta^2 \frac{V_0}{V_0 + V_{\text{up}}} e^{-\beta\phi}. \quad (50)$$

Substituting the  $N$ - $\phi$  relation from Eq. (45), one finds

$$\epsilon_V \simeq \frac{3\alpha}{4N^2} \left( \frac{V_0}{V_0 + V_{\text{up}}} \right)^2, \quad \eta_V \simeq -\frac{1}{N}. \quad (51)$$

Hence, the scalar spectral index and tensor-to-scalar ratio at leading order are

$$n_s = 1 - 6\epsilon_V + 2\eta_V \simeq 1 - \frac{2}{N_*}, \quad r = 16\epsilon_V \simeq \frac{12\alpha}{N_*^2} \left( \frac{V_0}{V_0 + V_{\text{up}}} \right)^2. \quad (52)$$

These results reproduce the universal  $\alpha$ -attractor predictions for  $n_s$ , while introducing a controlled suppression of  $r$  through the uplift factor. For  $V_{\text{up}} = 0$ , Eq. (52) reduces to the standard E-model relation, confirming consistency with the pure attractor limit.

### Finite- $N$ and uplift corrections

The full expression (44) can be used to compute subleading corrections to the observables. Expanding in powers of  $1/u$  and  $V_{\text{up}}/V_0$  yields

$$n_s = 1 - \frac{2}{N_*} - \frac{3}{2N_*^2} \frac{V_{\text{up}}}{V_0 + V_{\text{up}}} + \mathcal{O}(N_*^{-3}), \quad r = \frac{12\alpha}{N_*^2} \left( \frac{V_0}{V_0 + V_{\text{up}}} \right)^2 \left[ 1 - \frac{2}{N_*} \frac{V_{\text{up}}}{V_0 + V_{\text{up}}} \right]. \quad (53)$$

These small deviations are numerically negligible for  $V_{\text{up}} \lesssim 0.3V_0$  but can become relevant if the uplift dominates the plateau energy density.

Figure 2 in Sec. VI illustrates how these analytical results match the numerical solutions of the full background equations, confirming that the uplift merely rescales the tensor amplitude while preserving the tilt- $N_*$  relation to high precision.

## IV. Perturbations and quantum consistency

### Hubble-flow hierarchy and next-to-leading order spectra

The evolution of inflationary fluctuations can be described in a model-independent manner using the Hubble-flow hierarchy [85],

$$\epsilon_1 \equiv -\frac{\dot{H}}{H^2}, \quad \epsilon_{n+1} \equiv \frac{d \ln \epsilon_n}{dN}, \quad (54)$$

where  $N = \ln a$  denotes the number of e-folds. The first parameter  $\epsilon_1$  measures the fractional rate of change of the Hubble parameter, and inflation persists for  $\epsilon_1 < 1$ . Higher  $\epsilon_n$  capture successive logarithmic derivatives and organize the slow-roll expansion to arbitrary order.

For the hybrid  $\alpha$ -attractor potential  $V = U + V_{\text{up}}$ , the background identity

$$\frac{d\phi}{dN} = -\frac{U'(\phi)}{U(\phi) + V_{\text{up}}}, \quad (55)$$

holds exactly, leading to

$$\epsilon_1 = \frac{1}{2} \left( \frac{d\phi}{dN} \right)^2 = \frac{1}{2} \left( \frac{U'(\phi)}{V(\phi)} \right)^2, \quad (56)$$

which coincides with  $\epsilon_V$  only to first order in slow roll. Beyond leading order, replacing  $\epsilon_1$  with  $\epsilon_V$  in the Stewart–Lyth expressions leads to  $\mathcal{O}(\epsilon^2)$  inconsistencies. Hence, all observables are computed using the exact background relation  $d\phi/dN = -U'/V$  and the numerical  $\epsilon_n(N)$  hierarchy derived from Eq. (44).

At next-to-leading order (NLO) in the Stewart–Lyth expansion [72], the scalar and tensor power spectra evaluated at the pivot scale  $k_*$  are

$$\mathcal{P}_\zeta(k_*) = \frac{H_*^2}{8\pi^2 \epsilon_{1*}} [1 - (2\tilde{C} + 1)\epsilon_{1*} - \tilde{C}\epsilon_{2*}] + \mathcal{O}(\epsilon^2), \quad (57)$$

$$n_s = 1 - 2\epsilon_{1*} - \epsilon_{2*} - 2\epsilon_{1*}^2 - (2\tilde{C} + 3)\epsilon_{1*}\epsilon_{2*} - \tilde{C}\epsilon_{2*}\epsilon_{3*} + \mathcal{O}(\epsilon^3), \quad (58)$$

$$r = 16\epsilon_{1*} [1 + \tilde{C}(\epsilon_{2*} - 2\epsilon_{1*})], \quad (59)$$

$$n_t = -2\epsilon_{1*} - 2(1 + \tilde{C})\epsilon_{1*}\epsilon_{2*} + \mathcal{O}(\epsilon^3), \quad (60)$$

where  $\tilde{C} = -2 + \ln 2 + \gamma_E \simeq -0.7296$ . These yield the NLO single-field consistency relation

$$r = -8n_t \left[ 1 - \frac{1 + \tilde{C}}{2} n_t + \frac{\tilde{C}}{2} (n_s - 1) \right] + \mathcal{O}(10^{-3}), \quad (61)$$

reducing to  $r = -8n_t$  at leading order. The initial conditions are set by the Bunch–Davies vacuum,  $v_k \rightarrow e^{-ik\tau}/\sqrt{2k}$  as  $k|\tau| \rightarrow \infty$  [86].

The uplift  $V_{\text{up}}$  primarily rescales  $V$ , suppressing  $\epsilon_1$  by  $(V_0/(V_0 + V_{\text{up}}))^2$  and slightly modifying  $\epsilon_2$ , thereby reducing  $r$  without significantly shifting  $n_s$ . This behavior confirms the robustness of the  $\alpha$ -attractor prediction  $n_s \simeq 1 - 2/N_*$  with a mildly reduced tensor amplitude.

### Classicality and radiative stability

Quantum diffusion is negligible when the classical field displacement per e-fold dominates over stochastic fluctuations,

$$\epsilon_V(\phi) > \frac{V(\phi)}{24\pi^2}. \quad (62)$$

On the E-model plateau,  $U \rightarrow V_0$  and  $\epsilon_V \propto e^{-2\beta\phi}$ , making the inequality (62) easily satisfied throughout the observable regime. For  $\alpha \lesssim 1$  and  $V_0^{1/4} \sim 10^{-3}$ , one finds  $\epsilon_V \sim 10^{-4}\text{--}10^{-5}$  and  $V/(24\pi^2) \sim 10^{-11}$ , confirming

classical dominance and precluding self-reproduction. A full Langevin analysis [87, 88] yields the same conclusion up to higher-order slow-roll corrections.

Radiative stability follows from the exponentially suppressed Coleman–Weinberg slope on the plateau. The field-dependent masses of the waterfall multiplets are

$$m_{\pm}^2(\phi) = g^2|1 - e^{-\beta\phi}|^2 \pm g_X^2 v_D^2 + \Delta m^2(\phi), \quad m_F^2(\phi) = g^2|1 - e^{-\beta\phi}|^2, \quad (63)$$

and the one-loop correction in the  $\overline{\text{MS}}$  scheme reads [76]

$$\Delta V_{\text{CW}}(\phi) = \frac{1}{64\pi^2} \sum_i (-1)^{F_i} m_i^4(\phi) \left[ \ln \frac{m_i^2(\phi)}{\mu^2} - c_i \right]. \quad (64)$$

Because  $|1 - e^{-\beta\phi}| \rightarrow 1$  exponentially fast,  $\Delta V'_{\text{CW}} \propto e^{-\beta\phi}$ , and the loop-induced slope is negligible. Choosing  $\mu \sim m_F$  minimizes large logarithms. For  $g \lesssim 10^{-2}$ , loop corrections remain subpercent over the observable window, with only a tiny shift  $\phi_c \rightarrow \phi_c + \delta\phi_c$  ( $|\delta\phi_c| \ll \beta^{-1}$ ) in the critical point. The sequestered uplift sector does not contribute radiative instabilities, ensuring the plateau's technical naturalness.

## V. Post-inflationary dynamics and vacuum structure

### Reheating and $N_*-k_*$ mapping

Entropy-conserving matching relates the number of e-folds  $N_*$  to the pivot scale  $k_*$  [89, 90],

$$N_* \simeq 57 - \ln \frac{k_*}{0.05 \text{ Mpc}^{-1}} + \frac{1}{4} \ln \frac{V_*}{(10^{16} \text{ GeV})^4} + \frac{1}{4} \ln \frac{V_*}{V_{\text{end}}} + \frac{1 - 3w_{\text{reh}}}{12(1 + w_{\text{reh}})} \ln \frac{\rho_{\text{reh}}}{\rho_{\text{end}}}. \quad (65)$$

Inflation ends when  $m_-^2(\phi_c) = 0$ , with

$$V_{\text{end}} = U(\phi_c) + V_{\text{up}}. \quad (66)$$

The energy difference  $\Delta V = V_{\text{end}} - V_{\text{vac}}$  drives reheating. For perturbative decays with total width  $\Gamma$ , the reheating temperature is

$$T_{\text{RH}} \simeq \left( \frac{90}{\pi^2 g_*} \right)^{1/4} \sqrt{\Gamma M_{\text{Pl}}} \quad (\text{e.g. } \Gamma \simeq y^2 m / (8\pi) \text{ for Yukawa portals}), \quad (67)$$

while non-perturbative mechanisms (parametric resonance or tachyonic preheating) can be parametrized effectively through  $(w_{\text{reh}}, \rho_{\text{reh}})$  [91]. The resulting uncertainty in  $N_*$  induces only mild shifts in  $(n_s, r)$  due to the attractor scaling  $r \propto N_*^{-2}$ .

### Stabilization, topological defects, and vacuum tuning

Orthogonal stabilization of the field  $S$  is achieved by a quartic Kähler correction,

$$K \supset (T + \bar{T})^{-3\alpha} (|S|^2 - \kappa_S |S|^4), \quad \kappa_S \gtrsim 1, \quad (68)$$

leading to

$$m_S^2 = c_S H^2 + \mathcal{O}(e^{-\sqrt{24\alpha}\phi}), \quad c_S = \mathcal{O}(\kappa_S). \quad (69)$$

Alternatively,  $S$  may be taken nilpotent ( $S^2 = 0$ ) [92], eliminating the scalar partner while preserving the uplift.

Since the gauged  $U(1)_X$  symmetry breaks during the waterfall, cosmic strings may form with tension  $\mu \simeq \pi v_D^2$ , corresponding to  $G\mu \simeq \pi v_D^2$ . Observational bounds  $G\mu \lesssim 10^{-7}\text{--}10^{-8}$  [4, 93] imply  $v_D \lesssim \mathcal{O}(10^{-4})$ . The uplift  $U(1)_D$  remains sequestered from the waterfall fields and produces no defects. The inflaton phase  $\text{Im } T$  stays light (see Eq. (25)); if necessary, small explicit stabilization terms can ensure a strictly single-field trajectory.

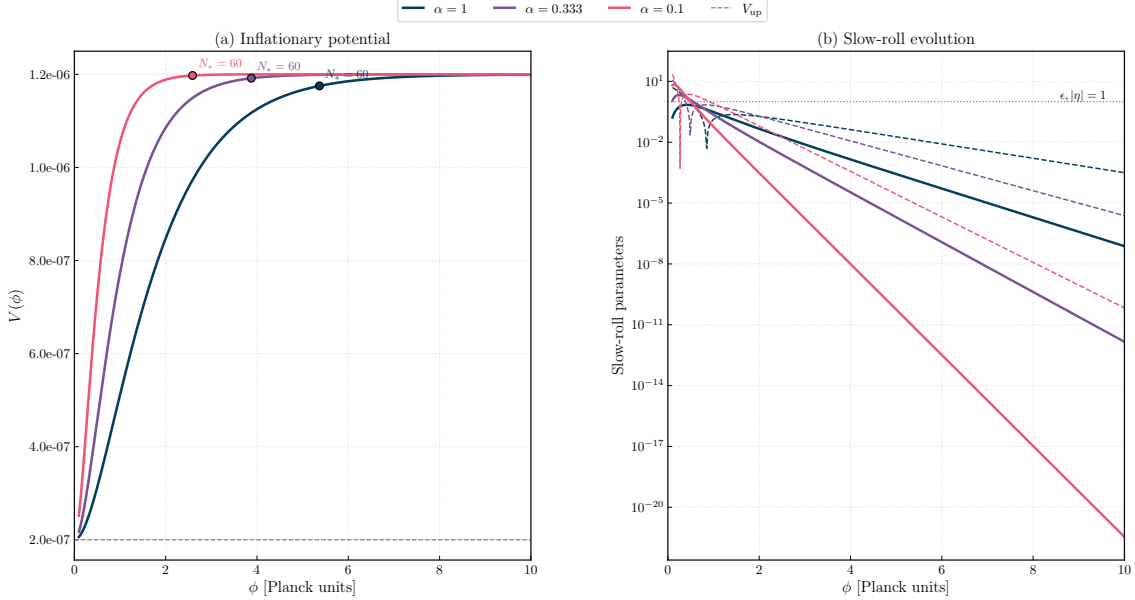


FIG. 1. The hybrid  $\alpha$ -attractor potential and its corresponding slow-roll parameters for  $\alpha = 1.0, 1/3$ , and  $0.1$ . **(Left)** The potential  $V(\phi) = V_0(1 - e^{-\beta\phi})^2 + V_{\text{up}}$  asymptotically approaches a plateau for large  $\phi$ , with smaller  $\alpha$  producing a flatter shape. The dashed line denotes the uplift term  $V_{\text{up}}$ , while the markers indicate the field values corresponding to  $N_* = 60$  e-folds before the end of inflation. **(Right)** The slow-roll parameters  $\epsilon(\phi)$  (solid) and  $|\eta(\phi)|$  (dashed) shown in logarithmic scale demonstrate that inflation persists as long as  $\epsilon, |\eta| \ll 1$ . Smaller  $\alpha$  values sustain a longer slow-roll regime, characteristic of plateau-like inflationary models.

After the waterfall, the vacuum energy becomes

$$V_{\text{vac}} = V_{\text{up}}^{\text{eff}} - \frac{g_X^2 v_D^4}{2}, \quad (70)$$

where  $V_{\text{up}}^{\text{eff}}$  includes any residual constant offset. A Minkowski vacuum requires  $V_{\text{up}}^{\text{eff}} = g_X^2 v_D^4/2$ , while small detuning yields a residual (A)dS state. This tuning affects only the late-time cosmological constant and remains independent of the inflationary observables, which depend solely on  $U(\phi)$  and  $V_{\text{up}}$  during the slow-roll phase.

## VI. Comparison with observations and parameter dependence

Figure 1 illustrates the behavior of the hybrid  $\alpha$ -attractor potential and its corresponding slow-roll dynamics in supergravity for three representative values of the Kähler curvature parameter,  $\alpha = 1.0, 1/3$ , and  $0.1$ . As shown in the left panel, the potential  $V(\phi) = V_0(1 - e^{-\beta\phi})^2 + V_{\text{up}}$  asymptotically approaches a plateau for large field values, a defining feature of  $\alpha$ -attractor models. Smaller values of  $\alpha$  lead to a flatter plateau and therefore an extended period of slow-roll inflation. The dashed horizontal line denotes the uplift contribution  $V_{\text{up}}$ , while the labeled points correspond to the field values at which approximately  $N_* = 60$  e-folds remain before the end of inflation, corresponding to the observable CMB pivot scales. The right panel of Fig. 1 shows the slow-roll parameters  $\epsilon(\phi)$  and  $|\eta(\phi)|$  as functions of  $\phi$ . Both quantities decrease exponentially along the inflationary plateau, confirming the near-constant Hubble rate during inflation. Inflation terminates when either  $\epsilon$  or  $|\eta|$  approaches unity, indicated by the dotted horizontal line. As  $\alpha$  decreases, both slow-roll parameters remain suppressed over a larger field range, leading to smaller tensor-to-scalar ratios and enhanced agreement with current observational constraints on inflationary models.

Figure 2 summarizes the predictions of the hybrid  $\alpha$ -attractor model with constant uplift in the  $(n_s, r)$  plane for representative choices of  $(\alpha, f)$  at  $N_* = 50$  and  $60$ . The dimensionless ratio

$$f \equiv \frac{V_0}{V_0 + V_{\text{up}}} \in (0, 1] \quad (71)$$

Model	$N_*$	$(n_s, r)$
Hybrid $\alpha$ -attractor ( $\alpha = 1.0, f = 1.0$ )	50	(0.961913, 0.004114)
	60	(0.968070, 0.002918)
Hybrid $\alpha$ -attractor ( $\alpha = 1.0, f = 0.7$ )	50	(0.961396, 0.004274)
	60	(0.967679, 0.003018)
Hybrid $\alpha$ -attractor ( $\alpha = 1/3, f = 1.0$ )	50	(0.961228, 0.001474)
	60	(0.967547, 0.001036)
Hybrid $\alpha$ -attractor ( $\alpha = 1/3, f = 0.7$ )	50	(0.960966, 0.001500)
	60	(0.967353, 0.001052)
Hybrid $\alpha$ -attractor ( $\alpha = 0.1, f = 1.0$ )	50	(0.960847, 0.000457)
	60	(0.967263, 0.000320)
Hybrid $\alpha$ -attractor ( $\alpha = 0.1, f = 0.7$ )	50	(0.960737, 0.000460)
	60	(0.967184, 0.000322)

TABLE I. Numerical  $(n_s, r)$  benchmarks used in Fig. 2. The results exhibit the universal  $n_s$ – $N_*$  attractor behaviour and a mild, controlled  $f$ -dependence of  $r$  once the exact  $N(\phi)$  mapping and hybrid exit are included.

measures the fraction of the total plateau energy contributed by the inflaton sector. The limit  $f \rightarrow 1$  corresponds to vanishing uplift, while smaller  $f$  represents a more strongly sequestered de Sitter offset.

The plateau dynamics reproduce the universal  $\alpha$ -attractor relation

$$n_s \simeq 1 - \frac{2}{N_*}, \quad r \simeq \frac{12\alpha}{N_*^2} f^2 + \mathcal{O}\left(\frac{1}{N_*^3}\right), \quad (72)$$

with only mild finite- $N$  corrections once the exact  $N(\phi)$  mapping from Eq. (44) and the hybrid exit condition are included. The numerical results in Table I confirm these analytic expectations and illustrate the dependence on  $(\alpha, f, N_*)$ :

- × **Scalar tilt.** Across all benchmarks and e-fold values,  $n_s$  remains anchored to  $1 - 2/N_*$ , yielding  $n_s \simeq 0.962$  for  $N_* = 50$  and  $n_s \simeq 0.968$  for  $N_* = 60$ . This agrees with Planck’s preferred red tilt and demonstrates that the uplifted hybrid construction preserves the universal  $\alpha$ -attractor scaling.
- × **Tensor amplitude.** Decreasing  $\alpha$  lowers  $r$  nearly vertically in the  $(n_s, r)$  plane, from  $\mathcal{O}(10^{-3})$  for  $\alpha = 1$  to  $\mathcal{O}(10^{-4})$  for  $\alpha = 0.1$  at fixed  $N_*$ . The  $f$ -dependence is notably weaker than the naive  $f^2$  scaling in Eq. (72): reducing  $f$  from 1.0 to 0.7 changes  $r$  by only a few percent. This mild sensitivity arises because the uplift modifies both the exact  $N(\phi)$  relation and the Hubble-flow hierarchy, partially compensating the potential-height rescaling.
- × **E-fold dependence.** Increasing  $N_*$  from 50 to 60 raises  $n_s$  by  $\simeq 0.006$  and suppresses  $r$  roughly by  $(50/60)^2$ , in excellent agreement with Eq. (72). The near-universal clustering of points along  $n_s \simeq 1 - 2/N_*$  confirms that the attractor geometry is preserved even with uplift and hybrid termination.
- × **Observational viability.** All benchmarks lie within the 68% confidence contours of current CMB datasets (Planck, B18, DESI) and are consistent with LiteBIRD forecasts. For  $\alpha \leq 1$  at  $N_* = 60$ , the tensor amplitude satisfies  $r \lesssim 4 \times 10^{-3}$ , decreasing to  $r \simeq 3 \times 10^{-4}$  for  $\alpha = 0.1$ . The model thus comfortably evades present tensor bounds while remaining within reach of upcoming  $B$ -mode experiments.

The parameter trajectories in Fig. 2 illustrate how each variable controls the observables:  $\alpha$  predominantly sets the vertical scale of  $r$ ;  $f$  introduces a gentle upward bend through uplift corrections to  $N(\phi)$ ; and  $N_*$  moves predictions along the attractor track toward higher  $n_s$  and smaller  $r$ . All results cluster around the universal curve  $n_s \simeq 1 - 2/N_*$ , confirming that constant uplift preserves the core attractor symmetry while providing a controlled suppression of tensors.

## VII. Conclusion

We have developed a fully analytic and geometrically consistent realization of hybrid inflation within the framework of supergravity  $\alpha$ -attractors. Unlike previous constructions that relied on approximate attractor potentials or non-sequestered uplifting sectors, the present model incorporates an exactly constant uplift originating from a hidden

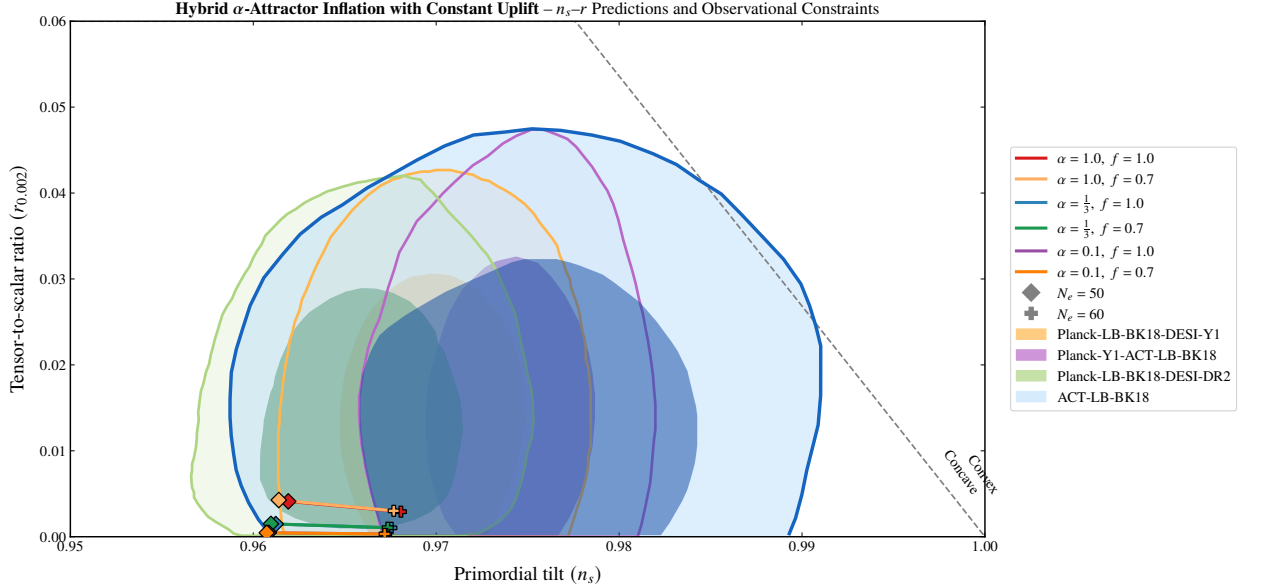


FIG. 2. Predictions of hybrid  $\alpha$ -attractor inflation with constant uplift. Points indicate  $N_* = 50$  and 60 for the benchmarks in Table I. Observational contours correspond to the combined Planck–LiteBIRD–BK18–DESI analysis. Decreasing  $\alpha$  suppresses  $r$  nearly vertically, while smaller  $f$  (stronger uplift) produces a mild upward shift. The universal scaling  $n_s \simeq 1 - 2/N_*$  is maintained throughout.

Stückelberg  $U(1)_D$  gauge sector. This uplift leaves the inflaton dynamics intact, ensuring that the slow-roll trajectory remains governed by the universal attractor geometry.

The symmetry-protected Kähler potential produces an exact E-model plateau

$$U(\phi) = V_0 (1 - e^{-\beta\phi})^2, \quad \beta = \sqrt{\frac{2}{3\alpha}},$$

while the constant uplift simply rescales the total energy density by a factor  $f = V_0/(V_0 + V_{\text{up}})$  without introducing backreaction. We derived a closed-form  $N\phi$  relation and exact expressions for the slow-roll hierarchy, allowing next-to-leading-order analytic predictions for the cosmological observables. The model reproduces the universal  $\alpha$ -attractor scaling

$$n_s \simeq 1 - \frac{2}{N_*}, \quad r \simeq \frac{12\alpha}{N_*^2} f^2,$$

with minimal corrections from the hybrid exit condition. For  $\alpha \leq 1$  and  $N_* = 60$ , we find  $n_s \simeq 0.968$  and  $r \lesssim 4 \times 10^{-3}$ , consistent with current Planck, BK18, and DESI data and within the reach of forthcoming  $B$ -mode polarization missions such as LiteBIRD and CMB-S4 [94, 95].

The sequestered uplift mechanism enables an independent tuning of the post-inflationary vacuum,

$$V_{\text{vac}} = V_{\text{up}}^{\text{eff}} - \frac{g_X^2 v_D^4}{2} \simeq 0,$$

thereby preserving radiative stability and preventing feedback on the slow-roll parameters. The suppression of the tensor amplitude  $r$  arises geometrically rather than through fine-tuning, rendering the framework robust, predictive, and falsifiable. The reheating phase is naturally controlled by the  $U(1)_X$  waterfall interactions, providing a consistent path toward the Standard Model sector.

Beyond the minimal setup explored here, several extensions merit further study. Embedding the sequestered uplift into string-theoretic moduli stabilization, for instance within KKLT- or LVS-type compactifications, could clarify how the effective parameter  $V_{\text{up}}$  emerges dynamically from hidden brane or flux sectors. A more detailed analysis of

reheating—including the coupling of the waterfall fields to visible-sector matter—would allow a direct link between the inflationary scale and the post-inflationary thermal history. Moreover, the suppressed tensor amplitude predicted here places the model squarely within the sensitivity range of LiteBIRD and CMB-S4, offering a decisive observational test of the geometric attractor paradigm in the near future.

The constant sequestered uplift employed in this work can arise naturally from ultraviolet completions. In type-IIB flux compactifications, D-term uplifts may originate from anomalous  $U(1)$  symmetries on magnetized D7-branes, while nilpotent F-term sources associated with anti-D3 branes at warped throats can generate similar effective contributions. In both cases, the resulting four-dimensional scalar potential includes a term of the form  $V_{\text{up}} = D/M_{\text{Pl}}^4$ , where  $D$  encodes the flux-induced supersymmetry-breaking scale. Because the uplift sector is sequestered, it preserves the inflaton geometry and does not spoil the  $\alpha$ -attractor predictions, making this mechanism fully compatible with the supergravity embedding presented here.

In conclusion, the hybrid  $\alpha$ -attractor with constant uplift provides a clean, analytic, and symmetry-protected framework for realizing inflation in supergravity. Its geometric suppression of tensor modes, radiative stability, and decoupled vacuum tuning make it a predictive and UV-consistent benchmark for future exploration and observational tests.

### Acknowledgments

The author would like to acknowledge that this work was conducted without external funding. The author appreciates the support of their academic community and peers for their valuable discussions and insights.

## Appendix A: Exact Hubble-flow hierarchy with constant uplift

This appendix presents a fully explicit derivation of the Hubble-flow hierarchy for the hybrid  $\alpha$ -attractor potential with a constant uplift term, retaining exact background dynamics without invoking the slow-roll approximation. The goal is to express the parameters  $\epsilon_1$ ,  $\epsilon_2$ , and  $\epsilon_3$  analytically in terms of the auxiliary field variable  $u \equiv e^{\beta\phi}$ , where  $\beta = \sqrt{2/(3\alpha)}$ . These expressions, combined with the Stewart–Lyth formulas of Sec. IV, enable next-to-leading-order (NLO) predictions for the spectral observables ( $n_s$ ,  $r$ ,  $n_t$ ) that remain valid even in regions where higher-order slow-roll corrections could be non-negligible.

### A.1 Setup and background relations

The inflaton potential in the Einstein frame, including a constant sequestered uplift  $V_{\text{up}}$ , is

$$V(\phi) = U(\phi) + V_{\text{up}}, \quad U(\phi) = V_0(1 - e^{-\beta\phi})^2. \quad (73)$$

To simplify the algebraic structure, we define

$$u \equiv e^{\beta\phi} \iff \phi = \frac{1}{\beta} \ln u, \quad (74)$$

so that derivatives with respect to  $\phi$  translate into derivatives with respect to  $u$  as

$$\frac{d}{d\phi} = \beta u \frac{d}{du}. \quad (75)$$

Expressed in terms of  $u$ , the potential and its derivative are

$$U(u) = V_0 \left( 1 - \frac{2}{u} + \frac{1}{u^2} \right), \quad U'(\phi) = \frac{dU}{d\phi} = 2V_0\beta \frac{u-1}{u^2}, \quad (76)$$

and the full scalar potential becomes

$$V(u) = V_0 \left( 1 - \frac{2}{u} + \frac{1}{u^2} \right) + V_{\text{up}}. \quad (77)$$

The exact background equation of motion in terms of e-fold time  $N = \ln a$  reads

$$\frac{d\phi}{dN} = -\frac{U'(\phi)}{V(\phi)}. \quad (78)$$

Using Eqs. (75) and (76), this implies

$$\frac{du}{dN} = \beta u \frac{d\phi}{dN} = -\frac{2\beta^2 V_0(u-1)}{u V(u)}. \quad (79)$$

Equation (79) constitutes the exact first-order background evolution equation in terms of  $u$ .

### A.2 First Hubble-flow parameter

The first Hubble-flow parameter  $\epsilon_1$  measures the fractional rate of change of  $H$ :

$$\epsilon_1 \equiv -\frac{\dot{H}}{H^2} = \frac{1}{2} \left( \frac{d\phi}{dN} \right)^2. \quad (80)$$

Substituting Eq. (78), we obtain the exact expression

$$\begin{aligned} \epsilon_1 &= \frac{1}{2} \left( \frac{U'(\phi)}{V(\phi)} \right)^2 = \frac{1}{2} \left( \frac{2V_0\beta(u-1)/u^2}{V(u)} \right)^2 \\ &= \frac{2\beta^2 V_0^2 (u-1)^2}{u^4 V(u)^2}. \end{aligned} \quad (81)$$

In the large-field limit  $u \gg 1$ , this reduces to  $\epsilon_1 \simeq 2\beta^2 V_0^2 / V^2 u^{-2}$ , recovering the expected exponential suppression on the plateau.

### A.3 Second Hubble-flow parameter

The next parameter is defined recursively as

$$\epsilon_2 \equiv \frac{d \ln \epsilon_1}{dN} = \frac{1}{\epsilon_1} \frac{d\epsilon_1}{du} \frac{du}{dN}. \quad (82)$$

Differentiating Eq. (81) with respect to  $u$  yields

$$\frac{d\epsilon_1}{du} = \epsilon_1 \left[ \frac{2}{u-1} - \frac{4}{u} - 2 \frac{V_u}{V} \right], \quad V_u \equiv \frac{dV}{du} = \frac{2V_0(u-1)}{u^3}. \quad (83)$$

Combining Eqs. (82) and (83) gives

$$\epsilon_2 = \left[ \frac{2}{u-1} - \frac{4}{u} - \frac{2V_u}{V} \right] \frac{du}{dN}. \quad (84)$$

Using Eq. (79) to substitute  $du/dN$ , we arrive at an explicit closed-form expression:

$$\epsilon_2 = -\frac{2\beta^2 V_0(u-1)}{u V} \left[ \frac{2}{u-1} - \frac{4}{u} - \frac{4V_0(u-1)}{u^3 V} \right]. \quad (85)$$

This relation is exact and valid for all field values along the inflationary valley. It can be evaluated either analytically or numerically without assuming small  $\epsilon_1$ .

A useful check comes from taking the asymptotic limit  $u \gg 1$ , where  $V \simeq V_0 + V_{\text{up}}$  and  $u-1 \simeq u$ :

$$\epsilon_2 \simeq -\frac{4\beta^2 V_0}{V} \left( 1 - \frac{V_0}{V} \right) \simeq -2\epsilon_1, \quad (86)$$

which reproduces the leading slow-roll scaling and confirms internal consistency.

#### A.4 Third Hubble-flow parameter

The third member of the hierarchy, required for the full NLO expressions of  $n_s$  and  $r$ , is

$$\epsilon_3 \equiv \frac{d \ln \epsilon_2}{dN} = \left( \frac{1}{\epsilon_2} \frac{d\epsilon_2}{du} \right) \frac{du}{dN}. \quad (87)$$

Differentiating Eq. (85) with respect to  $u$  gives

$$\frac{d\epsilon_2}{du} = -\frac{2\beta^2 V_0}{V} \left[ \frac{(u-1)}{u} \frac{d}{du} \left( \frac{2}{u-1} - \frac{4}{u} - \frac{4V_0(u-1)}{u^3 V} \right) + \frac{d}{du} \left( \frac{(u-1)}{uV} \right) \left( 2 - \frac{4(u-1)}{u} - \frac{4V_0(u-1)^2}{u^3 V} \right) \right], \quad (88)$$

which can be simplified algorithmically or implemented symbolically in numerical codes. Substituting into Eq. (87) with Eq. (79) yields an explicit form for  $\epsilon_3(N)$ .

In practice,  $\epsilon_3$  remains numerically small ( $|\epsilon_3| \lesssim 10^{-2}$ ) across the observable window for typical  $(\alpha, f)$ , confirming the validity of the NLO truncation.

#### A.5 Observables from the exact hierarchy

The full hierarchy  $\{\epsilon_1, \epsilon_2, \epsilon_3\}$  obtained above can be directly inserted into the Stewart–Lyth expressions of Sec. IV:

$$\mathcal{P}_\zeta(k_*) = \frac{H_*^2}{8\pi^2 \epsilon_{1*}} \left[ 1 - (2\tilde{C} + 1)\epsilon_{1*} - \tilde{C}\epsilon_{2*} \right], \quad (89)$$

$$n_s = 1 - 2\epsilon_{1*} - \epsilon_{2*} - 2\epsilon_{1*}^2 - (2\tilde{C} + 3)\epsilon_{1*}\epsilon_{2*} - \tilde{C}\epsilon_{2*}\epsilon_{3*}, \quad (90)$$

$$r = 16\epsilon_{1*} \left[ 1 + \tilde{C}(\epsilon_{2*} - 2\epsilon_{1*}) \right], \quad (91)$$

where  $\tilde{C} = -2 + \ln 2 + \gamma_E \simeq -0.7296$  and all quantities are evaluated at the pivot  $k_* = a_* H_*$ . By integrating Eq. (79) from the critical point  $u_c = e^{\beta\phi_c}$  to  $u_*$  corresponding to  $N_*$ , one can determine  $\epsilon_n(N_*)$  exactly, and hence obtain  $n_s$  and  $r$  to NLO without assuming  $\epsilon_n \ll 1$  for the background.

#### A.6 Numerical implementation and consistency checks

In practical computations, it is advantageous to integrate Eq. (79) numerically with initial condition  $u = u_c$  at  $N = 0$ , incrementing  $N$  until  $N = N_*$  corresponding to the desired horizon-crossing point. At each step,  $\epsilon_1(u)$ ,  $\epsilon_2(u)$ , and  $\epsilon_3(u)$  can be evaluated from Eqs. (81)–(87). This guarantees internal consistency between the background evolution and the perturbative expansion.

Consistency with the slow-roll limit can be verified by expanding the exact expressions at large  $u$ :

$$\epsilon_1 \simeq \frac{2\beta^2 V_0^2}{V^2} e^{-2\beta\phi}, \quad \epsilon_2 \simeq 4\beta^2 \frac{V_0^2}{V^2} e^{-2\beta\phi}, \quad \epsilon_3 \simeq 0, \quad (92)$$

which reproduce the standard results for E-model  $\alpha$ -attractors when  $V_{\text{up}} \rightarrow 0$ . The inclusion of the constant uplift therefore modifies only the overall normalization of the potential and the mapping between  $\phi$  and  $N$ , while preserving the asymptotic exponential suppression that ensures slow roll.

For convenience, the hierarchy is collected below in compact analytic form:

$$\begin{aligned} \epsilon_1 &= \frac{2\beta^2 V_0^2}{V(u)^2} \frac{(u-1)^2}{u^4}, \\ \epsilon_2 &= -\frac{2\beta^2 V_0(u-1)}{u V(u)} \left[ \frac{2}{u-1} - \frac{4}{u} - \frac{4V_0(u-1)}{u^3 V(u)} \right], \\ \epsilon_3 &= \left( \frac{1}{\epsilon_2} \frac{d\epsilon_2}{du} \right) \left[ -\frac{2\beta^2 V_0(u-1)}{u V(u)} \right]. \end{aligned} \quad (93)$$

These relations, together with Eq. (79), provide a fully self-contained and exact description of the background and perturbation hierarchy in the hybrid  $\alpha$ -attractor model with constant uplift. They constitute the analytic foundation for the numerical results and  $(n_s, r)$  predictions summarized in Sec. VI.

---

\* swapnilsingh.ph@gmail.com (Corresponding author)

- [1] A. H. Guth, “Inflationary universe: A possible solution to the horizon and flatness problems,” *Phys. Rev. D* **23** (1981) 347.
- [2] A. D. Linde, “A new inflationary universe scenario: A possible solution of the horizon, flatness, homogeneity, isotropy and primordial monopole problems,” *Phys. Lett. B* **108** (1982) 389.
- [3] A. Albrecht and P. J. Steinhardt, “Cosmology for grand unified theories with radiatively induced symmetry breaking,” *Phys. Rev. Lett.* **48** (1982) 1220.
- [4] **Planck** Collaboration, Y. Akrami *et al.*, “Planck 2018 results. X. Constraints on inflation,” *Astron. Astrophys.* **641** (2020) A10, [arXiv:1807.06211 \[astro-ph.CO\]](https://arxiv.org/abs/1807.06211).
- [5] **Planck** Collaboration, N. Aghanim *et al.*, “Planck 2018 results. VI. Cosmological parameters,” *Astron. Astrophys.* **641** (2020) A6, [arXiv:1807.06209 \[astro-ph.CO\]](https://arxiv.org/abs/1807.06209). [Erratum: *Astron. Astrophys.* 652, C4 (2021)].
- [6] **Simons Observatory** Collaboration, M. H. Abitbol *et al.*, “The Simons Observatory: Astro2020 Decadal Project Whitepaper,” *Bull. Am. Astron. Soc.* **51** (2019) 147, [arXiv:1907.08284 \[astro-ph.IM\]](https://arxiv.org/abs/1907.08284).
- [7] E. A. et al. [LiteBIRD], “Probing cosmic inflation with the litebird cosmic microwave background polarization survey,” *PTEP* **2023** no. 4, (2023) 042F01, [arXiv:2202.02773 \[astro-ph.IM\]](https://arxiv.org/abs/2202.02773).
- [8] S. H. et al., “Sensitivity studies for third-generation gravitational wave observatories,” *Class. Quant. Grav.* **28** (2011) 094013, [arXiv:1012.0908 \[gr-qc\]](https://arxiv.org/abs/1012.0908).
- [9] J. B. et al., “The laser interferometer space antenna: Unveiling the millihertz gravitational wave sky.”
- [10] T. L. Smith and R. Caldwell, “Lisa for cosmologists: Calculating the signal-to-noise ratio for stochastic and deterministic sources,” *Phys. Rev. D* **100** no. 10, (2019) 104055, [arXiv:1908.00546 \[astro-ph.CO\]](https://arxiv.org/abs/1908.00546).
- [11] J. Crowder and N. J. Cornish, “Beyond lisa: Exploring future gravitational wave missions,” *Phys. Rev. D* **72** (2005) 083005, [arXiv:gr-qc/0506015 \[gr-qc\]](https://arxiv.org/abs/gr-qc/0506015).
- [12] T. L. Smith and R. Caldwell, “Sensitivity to a frequency-dependent circular polarization in an isotropic stochastic gravitational wave background,” *Phys. Rev. D* **95** no. 4, (2017) 044036, [arXiv:1609.05901 \[gr-qc\]](https://arxiv.org/abs/1609.05901).
- [13] N. Seto, S. Kawamura, and T. Nakamura, “Possibility of direct measurement of the acceleration of the universe using 0.1-hz band laser interferometer gravitational wave antenna in space,” *Phys. Rev. Lett.* **87** (2001) 221103, [arXiv:astro-ph/0108011 \[astro-ph\]](https://arxiv.org/abs/astro-ph/0108011).
- [14] S. K. et al., “Current status of space gravitational wave antenna decigo and b-decigo.”
- [15] A. W. et al., “Fundamental physics with the square kilometre array,” *Publ. Astron. Soc. Austral.* **37** (2020) e002, [arXiv:1810.02680 \[astro-ph.CO\]](https://arxiv.org/abs/1810.02680).
- [16] **LISA Cosmology Working Group** Collaboration, P. Auclair *et al.*, “Cosmology with the Laser Interferometer Space Antenna,” [arXiv:2204.05434 \[astro-ph.CO\]](https://arxiv.org/abs/2204.05434).
- [17] **NANOGrav** Collaboration, G. Agazie *et al.*, “The NANOGrav 15 yr Data Set: Evidence for a Gravitational-wave Background,” *Astrophys. J. Lett.* **951** no. 1, (2023) L8, [arXiv:2306.16213 \[astro-ph.HE\]](https://arxiv.org/abs/2306.16213).
- [18] J. A. et al., “The second data release from the european pulsar timing array iii: Search for gravitational wave signals.”
- [19] D. J. Reardon *et al.*, “Search for an Isotropic Gravitational-wave Background with the Parkes Pulsar Timing Array,” *Astrophys. J. Lett.* **951** no. 1, (2023) L6, [arXiv:2306.16215 \[astro-ph.HE\]](https://arxiv.org/abs/2306.16215).
- [20] H. Xu *et al.*, “Searching for the Nano-Hertz Stochastic Gravitational Wave Background with the Chinese Pulsar Timing Array Data Release I,” *Res. Astron. Astrophys.* **23** no. 7, (2023) 075024, [arXiv:2306.16216 \[astro-ph.HE\]](https://arxiv.org/abs/2306.16216).
- [21] S. Vagnozzi, “Inflationary interpretation of the stochastic gravitational wave background signal detected by pulsar timing array experiments,” *JHEAp* **39** (2023) 81–98, [arXiv:2306.16912 \[astro-ph.CO\]](https://arxiv.org/abs/2306.16912).
- [22] V. K. Oikonomou, “Flat energy spectrum of primordial gravitational waves versus peaks and the nanograv 2023 observation,” *Phys. Rev. D* **108** no. 4, (2023) 043516, [arXiv:2306.17351 \[astro-ph.CO\]](https://arxiv.org/abs/2306.17351).
- [23] T. L. et al. [ACT], “The atacama cosmology telescope: Dr6 power spectra, likelihoods and  $\lambda$ cdm parameters.”
- [24] E. C. et al. [ACT], “The atacama cosmology telescope: Dr6 constraints on extended cosmological models.”
- [25] A. G. A. et al. [DESI], “Desi 2024 iii: Baryon acoustic oscillations from galaxies and quasars,” *JCAP* **04** (2025) 012, [arXiv:2404.03000 \[astro-ph.CO\]](https://arxiv.org/abs/2404.03000).
- [26] A. Addazi, Y. Aldabergenov, and S. V. Ketov, “Curvature corrections to Starobinsky inflation can explain the ACT results,” [arXiv:2505.10305 \[gr-qc\]](https://arxiv.org/abs/2505.10305).
- [27] S. Aoki, H. Otsuka, and R. Yanagita, “Higgs-modular inflation.”
- [28] S. Brahma and J. Calderón-Figueroa, “Is the CMB revealing signs of pre-inflationary physics?,” [arXiv:2504.02746 \[astro-ph.CO\]](https://arxiv.org/abs/2504.02746).
- [29] C. T. Byrnes, M. Cortês, and A. R. Liddle, “The curvaton acts again.”
- [30] S. Choudhury, G. Bauyrzhan, S. K. Singh, and K. Yerzhanov, “What new physics can we extract from inflation using the act dr6 and desi dr2 observations?.”
- [31] C. Dioguardi and A. Karam, “Palatini Linear Attractors Are Back in ACTion,” [arXiv:2504.12937 \[gr-qc\]](https://arxiv.org/abs/2504.12937).

[32] C. Dioguardi, A. J. Iovino, and A. Racioppi, “Fractional attractors in light of the latest act observations,” *Phys. Lett. B* **868** (2025) 139664, [arXiv:2504.02809 \[gr-qc\]](https://arxiv.org/abs/2504.02809).

[33] M. Drees and Y. Xu, “Refined Predictions for Starobinsky Inflation and Post-inflationary Constraints in Light of ACT,” [arXiv:2504.20757 \[astro-ph.CO\]](https://arxiv.org/abs/2504.20757).

[34] E. G. M. Ferreira, E. McDonough, L. Balkenhol, R. Kallosh, L. Knox, and A. Linde, “The bao-cmb tension and implications for inflation.”

[35] D. Frolovsky and S. V. Ketov, “Are single-field models of inflation and PBH production ruled out by ACT observations?,” [arXiv:2505.17514 \[astro-ph.CO\]](https://arxiv.org/abs/2505.17514).

[36] Q. Gao, Y. Gong, Z. Yi, and F. Zhang, “Non-minimal coupling in light of act.”

[37] Q. Gao, Y. Qian, Y. Gong, and Z. Yi, “Observational constraints on inflationary models with non-minimally derivative coupling by act.”

[38] I. D. Gialamas, A. Karam, A. Racioppi, and M. Raidal, “Has ACT measured radiative corrections to the tree-level Higgs-like inflation?,” [arXiv:2504.06002 \[astro-ph.CO\]](https://arxiv.org/abs/2504.06002).

[39] I. D. Gialamas, T. Katsoulas, and K. Tamvakis, “Keeping the relation between the Starobinsky model and no-scale supergravity ACTive,” [arXiv:2505.03608 \[gr-qc\]](https://arxiv.org/abs/2505.03608).

[40] M. Hai, A. R. Kamal, N. F. Shamma, and M. S. J. Shuvo, “Perturbative kähler moduli inflation.”

[41] R. Kallosh, A. Linde, and D. Roest, “A simple scenario for the last act.”

[42] G. Kouniatalis and E. N. Saridakis, “Inflation from a generalized exponential plateau: Towards extra suppressed tensor-to-scalar ratios.”

[43] L. Liu, Z. Yi, and Y. Gong, “Reconciling higgs inflation with act observations through reheating.”

[44] A. Mohammadi, Yogesh, and A. Wang, “Power law plateau inflation and primary gravitational waves in the light of act.”

[45] S. D. Odintsov and V. K. Oikonomou, “Gw170817 viable einstein-gauss-bonnet inflation compatible with the atacama cosmology telescope data,” *Phys. Lett. B* **868** (2025) 139779, [arXiv:2506.08193 \[gr-qc\]](https://arxiv.org/abs/2506.08193).

[46] Z. Z. Peng, Z. C. Chen, and L. Liu, “The polynomial potential inflation in light of act observations.”

[47] R. D. A. Q., J. Chagoya, and A. A. Roque, “Compact stars in einstein-scalar-gauss-bonnet gravity: Regular and divergent scalar field configurations.”

[48] A. Salvio, “Independent connection in ACTion during inflation,” [arXiv:2504.10488 \[hep-ph\]](https://arxiv.org/abs/2504.10488).

[49] W. J. Wolf, “Inflationary attractors and radiative corrections in light of act.”

[50] W. Yin, “Higgs-like inflation under activated mass.”

[51] Z. Yi, X. Wang, Q. Gao, and Y. Gong, “Potential reconstruction from act observations leading to polynomial  $\alpha$ -attractor.”

[52] Yogesh, A. Mohammadi, Q. Wu, and T. Zhu, “Starobinsky-like inflation and egb gravity in the light of act.”

[53] J. Yuennan, P. Koad, F. Atamurotov, and P. Channuie, “Quantum-corrected  $\phi^4$  inflation in light of act observations.”

[54] M. Zahoor, S. Khan, and I. A. Bhat, “Reconciling fractional power potential and egb gravity in the light of act.”

[55] Y. Zhu, Q. Gao, Y. Gong, and Z. Yi, “Inflationary models with gauss-bonnet coupling in light of act observations.”

[56] S. Aoki, H. Otsuka, and R. Yanagita, “Higgs-modular inflation,” 2025. <https://arxiv.org/abs/2504.01622>.

[57] A. Chakraborty, D. Maity, and R. Mondal, “Nonminimal infrared gravitational reheating in light of act,” 2025. <https://arxiv.org/abs/2506.02141>.

[58] R. Mondal, S. Mondal, and A. Chakraborty, “Constraining reheating temperature, inflaton-sm coupling and dark matter mass in light of act dr6 observations,” 2025. <https://arxiv.org/abs/2505.13387>.

[59] C. Pallis, “Kinetically modified palatini inflation meets act data,” 2025. <https://arxiv.org/abs/2505.23243>.

[60] W. J. Wolf, “Inflationary attractors and radiative corrections in light of act,” 2025. <https://arxiv.org/abs/2506.12436>.

[61] A. D. Linde, “Hybrid inflation,” *Phys. Rev. D* **49** (1994) 748–754, [astro-ph/9307002](https://arxiv.org/abs/astro-ph/9307002).

[62] E. J. Copeland, A. R. Liddle, D. H. Lyth, E. D. Stewart, and D. Wands, “False vacuum inflation with einstein gravity,” *Phys. Rev. D* **49** (1994) 6410, [astro-ph/9401011](https://arxiv.org/abs/astro-ph/9401011).

[63] G. R. Dvali, Q. Shafi, and R. K. Schaefer, “Large scale structure and supersymmetric inflation without fine tuning,” *Phys. Rev. Lett.* **73** (1994) 1886, [hep-ph/9406319](https://arxiv.org/abs/hep-ph/9406319).

[64] P. Binétruy and G. Dvali, “D-term inflation,” *Phys. Lett. B* **388** (1996) 241, [hep-ph/9606342](https://arxiv.org/abs/hep-ph/9606342).

[65] E. Halyo, “Hybrid inflation from supersymmetry breaking,” *Phys. Lett. B* **387** (1996) 43, [hep-ph/9606423](https://arxiv.org/abs/hep-ph/9606423).

[66] R. Kallosh and A. Linde, “Universality class in conformal inflation,” *JCAP* **1307** (2013) 002, [1306.5220](https://arxiv.org/abs/1306.5220).

[67] R. Kallosh and A. Linde, “Superconformal generalizations of the starobinsky model,” *JCAP* **1306** (2013) 028, [1306.3214](https://arxiv.org/abs/1306.3214).

[68] S. Ferrara, R. Kallosh, A. Linde, and M. Porrati, “Minimal supergravity models of inflation,” *Phys. Rev. D* **88** (2013) 085038, [1307.7696](https://arxiv.org/abs/1307.7696).

[69] M. Galante, R. Kallosh, A. Linde, and D. Roest, “Unity of cosmological inflation attractors,” *Phys. Rev. Lett.* **114** (2015) 141302, [1412.3797](https://arxiv.org/abs/1412.3797).

[70] A. Linde, “Single-field  $\alpha$ -attractors,” *JCAP* **1505** (2015) 003, [1504.00663](https://arxiv.org/abs/1504.00663).

[71] C. Pallis, “ACT-inspired Kähler-based inflationary attractors,” *JCAP* **09** (2025) 061, [arXiv:2507.02219 \[hep-ph\]](https://arxiv.org/abs/2507.02219).

[72] E. D. Stewart and D. H. Lyth, “A more accurate analytic calculation of the spectrum of cosmological perturbations produced during inflation,” *Phys. Lett. B* **302** (1993) 171–175, [gr-qc/9302019](https://arxiv.org/abs/gr-qc/9302019).

[73] S. M. Leach, A. R. Liddle, J. Martin, and D. J. Schwarz, “Cosmological parameter estimation and the inflationary cosmology,” *Phys. Rev. D* **66** (2002) 023515, [astro-ph/0202094](https://arxiv.org/abs/astro-ph/0202094).

[74] J.-O. Gong and E. D. Stewart, “The power spectrum for a multicomponent inflaton to second order corrections in the slow-roll expansion,” *Phys. Lett. B* **510** (2001) 1–9, [astro-ph/0101225](https://arxiv.org/abs/astro-ph/0101225).

[75] D. J. Schwarz, C. A. Terrero-Escalante, and A. A. Garcia, “Higher order corrections to primordial spectra from

cosmological inflation,” *Phys. Lett. B* **517** (2001) 243–249, [astro-ph/0106020](#).

[76] S. R. Coleman and E. J. Weinberg, “Radiative corrections as the origin of spontaneous symmetry breaking,” *Phys. Rev. D* **7** (1973) 1888–1910.

[77] R. Jackiw, “Functional evaluation of the effective potential,” *Phys. Rev. D* **9** (1974) 1686–1701.

[78] S. P. Martin, “Two-loop effective potential for a general renormalizable theory and softly broken supersymmetry,” *Phys. Rev. D* **65** (2002) 116003, [hep-ph/0111209](#).

[79] D. Roest *JHEP* **01** (2014) 007.

[80] R. Kallosh and A. Linde *JCAP* **12** (2015) 008.

[81] J. Wess and J. Bagger, *Supersymmetry and Supergravity*. Princeton University Press, 2 ed., 1992.

[82] D. Z. Freedman and A. Van Proeyen, *Supergravity*. Cambridge University Press, 2012.

[83] Z. Komargodski and N. Seiberg, “Comments on the fayet-iliopoulos term in field theory and supergravity,” *JHEP* **06** (2009) 007, [0904.1159](#).

[84] E. Dudas, S. Ferrara, A. Kehagias, and A. Sagnotti *JHEP* **06** (2014) 049.

[85] A. R. Liddle and D. H. Lyth, “Cobe, gravitational waves, inflation and extended inflation,” *Phys. Lett. B* **291** (1992) 391–398.

[86] T. S. Bunch and P. C. W. Davies *Proc. Roy. Soc. Lond. A* **360** (1978) 117.

[87] A. A. Starobinsky, “Stochastic de sitter (inflationary) stage in the early universe,” *Lect. Notes Phys.* **246** (1986) 107–126.

[88] A. D. Linde, “Eternally Existing Selfreproducing Chaotic Inflationary Universe,” *Phys. Lett. B* **175** (1986) 395–400.

[89] A. R. Liddle and S. M. Leach, “How long before the end of inflation were observable perturbations produced?” *Phys. Rev. D* **68** (2003) 103503, [astro-ph/0305263](#).

[90] L. Dai, M. Kamionkowski, and J. Wang, “Reheating constraints to inflationary models,” *Phys. Rev. Lett.* **113** (2014) 041302, [1404.6704](#).

[91] G. N. Felder, J. Garcia-Bellido, P. B. Greene, L. Kofman, A. Linde, and I. Tkachev, “Dynamics of symmetry breaking and tachyonic preheating,” *Phys. Rev. Lett.* **87** (2001) 011601, [hep-ph/0012142](#).

[92] S. Ferrara, R. Kallosh, and A. Linde *Phys. Rev. D* **90** (2014) 043541.

[93] J. J. Blanco-Pillado, K. D. Olum, and B. Shlaer *Phys. Rev. D* **89** (2014) 023512.

[94] M. Hazumi *et al.*, “Litebird: A satellite for the studies of b-mode polarization and inflation from cosmic background radiation detection,” *J. Low Temp. Phys.* **194** (2019) 443–452.

[95] K. N. Abazajian *et al.*, “Cmb-s4 science book, first edition,” [arXiv:1610.02743 \[astro-ph.CO\]](#).